

# Spectral-domain optical coherence tomography morphological characteristics in patients with cone dystrophy

Loh-Shan Leung (✉ [ibleung@stanford.edu](mailto:ibleung@stanford.edu))

Byers Eye Institute

Hassan Khojasteh

fatemeh bazvand

Farabi Eye Hospital, Eye Research Center, Tehran University of Medical Sciences

<https://orcid.org/0000-0001-9720-2028>

Mostafa Haidari

Alireza Mahmoudi

S. Saeed Mohammadi

Eye research center, Farabi eye hospital <https://orcid.org/0000-0002-5996-730X>

Hamid Riazi-Esfahani

Eye research center, Farabi eye hospital, Tehran, Iran <https://orcid.org/0000-0003-2277-398X>

Masoud Mirghorbani

Farabi eye hospital <https://orcid.org/0000-0003-4295-2563>

Arefeh Sheikholeslami Salmasi

Afsaneh Azarkish

Jonathan Regenold

<https://orcid.org/0000-0003-2138-515X>

Amir Akhavanrezayat

Irmak Karaca

Stanford University

Sung Who Park

Pusan National University Hospital <https://orcid.org/0000-0002-9186-2081>

Gunay Uludag

Byers Eye Institute, Stanford University

Chris Or

Hashem Ghoraba

Stanford University School of Medicine <https://orcid.org/0000-0002-1145-4134>

Quan Dong

Byers Eye Institute, Stanford Medicine <https://orcid.org/0000-0002-6024-8441>

## Article

**Keywords:** inherited retinal disorders, IRD, cone dystrophy, spectral-domain optical coherence tomography, SD-OCT

**Posted Date:** August 1st, 2023

**DOI:** <https://doi.org/10.21203/rs.3.rs-3079977/v1>

**License:**   This work is licensed under a Creative Commons Attribution 4.0 International License.

[Read Full License](#)

---

# Abstract

**Purpose:** To describe spectral-domain optical coherence tomography (SD-OCT) morphological characteristics in patients with cone dystrophy.

**Methods:** Forty-two patients (84 eyes) with the diagnosis of cone dystrophy based on clinical findings and electroretinogram reports (severely reduced or non-recordable cone response with preserved rod function) were included in our study. SD-OCT was performed and images were evaluated regarding the integrity and pattern of hyper-reflective outer retinal bands and other findings. The relationship between these findings, age, central subfoveal thickness (CST), and best-corrected visual acuity (BCVA) was assessed.

**Results:** 82 of 84 eyes (98 %) showed outer retinal layer abnormalities on SD-OCT. Five different morphological categories were identified on SD-OCT, including outer retinal atrophy (24.4%), undifferentiated outer retinal layers (22.0%), ellipsoid zone (EZ) disruption (19.5%), outer foveal defect (17.1%), and prominent outer retinal layers (17.1%). Also, five isolated OCT findings were detected, including foveal hypoplasia (14.6%), trans-retinal hyperreflective dots (THD) (29.3%), outer plexiform layer (OPL) schisis (11.3%), pseudodrusen (9.8%), and EZ bowing (13.4%). Age and CST were significantly different across the morphological categories ( $p < 0.001$ ). Eyes with prominent outer retinal layers and outer retinal atrophy had the best and worst visual acuity, respectively; however, the difference was not significant ( $p = 0.16$ ).

**Conclusion:** SD-OCT imaging shows variety of morphologic findings in cone dystrophy, which may be utilized in the assessment of these patients and may serve as predictive biomarkers for VA.

## Introduction

Cone dystrophy is a heterogeneous group of inherited retinal disorders (IRD) characterized by early onset progressive loss of vision, often accompanied by photophobia and hemeralopia.<sup>1</sup> Funduscopic findings of cone dystrophy range from a normal fundus appearance to bull's eye maculopathy, and the optic disc may show a variable degree of temporal pallor.<sup>2</sup> There are visual field defects such as reduced central sensitivity or relative scotoma with intact peripheral visual fields. Color vision might also be affected in all three axes.<sup>2</sup> In electroretinography (ERG), the cone response is reduced while the rod response is preserved, although in more advanced cases, the rod response may also be affected.<sup>2</sup> Several genes have been identified as carrying mutations that cause non-syndromic progressive cone degeneration.<sup>3</sup> The majority of these cases are autosomal recessive, but they can also be inherited as autosomal dominant or X-linked fashion.<sup>3</sup>

Optical coherence tomography (OCT) produces a cross-sectional image of the retina that enables structural evaluation and thickness measurements. By increasing the imaging speed in comparison to time-domain OCT, high-resolution spectral-domain optical coherence tomography (SD-OCT) provides a

higher axial resolution and less motion artifact.<sup>4</sup> Additionally, SD-OCT is a widely utilized imaging modality that is neither invasive nor technically challenging to use, making it as a practical method for diagnosing and monitoring the patients with cone dystrophy.<sup>5,6</sup> Nevertheless, there are few studies that evaluate specific structural changes in cone dystrophy using SD-OCT and their association with visual acuity (VA). Hood et al. reported decreased ellipsoid zone (EZ) intensity in 16 patients with cone dystrophy or achromatopsia.<sup>7</sup> Cho et al. evaluated 15 patients with cone dystrophy and reported four structural OCT categories: no abnormality, foveal EZ loss, foveal thinning with focal foveal EZ loss, and foveal thickening with perifoveal EZ disruption.<sup>8</sup> However, clinically, several other types of structural abnormalities may be observed that do not fall into these categories, most likely due to the diversity and heterogeneity of cone dystrophy genetic variants.

In the index study, we aimed to evaluate detailed SD-OCT findings of a large group of cone dystrophy patients and their correlation with visual function.

## Methods

### Patient selection

This retrospective observational study was conducted at a tertiary referral eye university hospital between July 2018 and September 2020. The study protocol was approved by the Tehran University of Medical Sciences Ethics Committee (approval code of IR.TUMS.FARABIH.REC.1398.035) and adhered to the Declaration of Helsinki tenets. All patients in this study had a history of hemeralopia, visual loss, or reduced color vision and underwent complete ophthalmological evaluation, full-field standard ERG testing, and SD-OCT imaging. The diagnosis of cone dystrophy was made using both clinical and electrophysiological findings.

### Clinical assessment and SD-OCT imaging

Ophthalmological examination included best-corrected visual acuity (BCVA) testing, recorded as the logarithm of the minimum angle of resolution (logMAR), slit-lamp examination, intraocular pressure measurement, and fundus examination. Full-field standard ERG was performed using the MonPack3 system (Metrovision, Pérenchies, France). The dark-adapted (DA) ERGs include responses to flash strengths (in photopic units; phot) of 0.01, 3 and 10 phot cd.s.m<sup>-2</sup> (DA 0.01; DA 3; DA 10). The light-adapted (LA) ERGs are to a flash strength of 3 phot cd.s.m<sup>-2</sup>, superimposed on a light-adapting background (luminance 30 cd.m<sup>-2</sup>) as single flashes (LA 3 ERG) and at a frequency of 30Hz (LA 30 Hz ERG). ERGs were performed in accordance with International Society for Clinical Electrophysiology of Vision (ISCEV) standards in an electrically shielded room to eliminate additional sound and background electrical noise.<sup>9</sup> All ERG tests were performed by an experienced examiner (H.K.). The ERG reports were reviewed and subjects with severely reduced or non-recordable cone responses and preserved rod function along with associated clinical findings were included in the study (Fig. 1).

All eyes were imaged using SD-OCT (Heidelberg Engineering, Heidelberg, Germany). SD-OCT images were reviewed and analyzed by two masked retina specialists (H.K. and F.B.). Any abnormality in retinal layers was reported and defined once both observers came to a consensus that it existed. Central subfoveal thickness (CST) was defined as the mean retinal thickness of the circular region surrounding the foveola measuring 1 mm in diameter.

## Statistical analysis

A Q-Q plot and Kolmogorov-Smirnov test were used to assess the normal distribution of data. To compensate for paired data regarding left and right eyes correlation (within subject correlation), we used generalized estimating equations (GEE) analysis to compare the age, CST, and VA between the five identified categories of retinal structural abnormalities. Post-hoc Sidak test was used in GEE analysis for pairwise comparison of different groups. Chi-square analysis was used to investigate the association between isolated signs and the five categories of retinal structural abnormalities on SD-OCT. Finally, a regression analysis was conducted to assess the possible relationship between VA of these patients and other variables.

Statistical analysis was performed using commercial software (SPSS ver. 26.0; SPSS Inc., Chicago, IL, USA). A p-value less than 0.05 was considered statistically significant.

## Results

A total of 42 patients were included in the study. 22/42 (53%) were female and the mean age of participants was  $21.3 \pm 15.3$  (range, 6–59) years old. The mean BCVA of patients was  $0.80 \pm 0.37$  LogMAR. The mean CST was  $191.22 \pm 52.76$   $\mu\text{m}$ . Patients included had no other neurologic or retinal abnormalities.

In SD-OCT evaluation, 40 patients showed retinal morphological changes in both of their eyes, while 2 patients presented with unilateral retinal changes; the normal fellow eyes had no OCT abnormalities. However, the corresponding full-field ERGs of these eyes showed reduced cone function. Analysis of the 82 eyes with SD-OCT abnormalities showed various retinal morphological changes. In the analysis of the four hyper-reflective outer retina bands, similar abnormalities were found between several eyes. Based on the qualitative concordance of the abnormal features, there were five categories of major retinal changes (Fig. 2); A) absence of external limiting membrane (ELM), ellipsoid zone (EZ), and interdigitation zone (IZ) leading to outward disfiguration of the retina, B) preserved ELM, EZ, and IZ that are not distinguishable or distinct (merging or hatching of layers), C) preserved ELM and IZ with scattered disruptions of the EZ, D) focal disruptions at any layer of ELM, EZ, or IZ at the foveola that create an optically empty space and E) preserved ELM, EZ, and IZ that are prominently hyper-reflective. These five categories in order of prevalence were 1- outer retinal atrophy (including diffuse outer retinal atrophy or waterfall - outward disfiguration) in 20 (24.4%) eyes, 2- undifferentiated outer retinal layers in 18 (22.0%) eyes, 3- EZ disruption in 16 (19.5%) eyes, 4- outer foveal defect in 14 (17.1%) eyes, and 5- prominent outer retinal

layers in 14 (17.1%) eyes (Fig. 2). The distribution of morphological changes between these 5 categories was relatively similar (from 17–24%;  $p = 0.9$ ). It is intriguing to note that both eyes of each individual showed symmetric morphological changes.

Furthermore, we observed several other abnormal structural morphologies on SD-OCT images of the cone dystrophy patients as isolated signs that can be found in any of the described major categories. These include foveal hypoplasia in 12 (14.6%) eyes, trans-retinal hyperreflective dots (THD) in 24 (29.3%) eyes, outer plexiform layer (OPL) schisis in 9 (11.3%) eyes, pseudodrusen in 8 (9.8%) eyes, and EZ bowing in 11 (13.4%) eyes (Fig. 3).

GEE analysis was used to assess the relationship between major morphological categories and age, VA, and CST (Table 1). There was a significant difference in age and CRT among morphological categories ( $p < 0.001$ ), while there was no statistically significant difference regarding BCVA ( $p = 0.09$ ). Patients whose SD-OCT images showed diffuse retinal atrophy had lower visual acuity (logMAR VA:  $0.96 \pm 0.39$ ) compared with other categories. In contrast, the prominent outer retinal layers group had a lesser effect on visual acuity (logMAR VA:  $0.65 \pm 0.33$ ). However, the difference of VA of these two groups was not statistically significant ( $p = 0.16$ ).

Table 1  
– Age, retinal thickness, and visual acuity among different morphological categories.

	Age (years)	CST ( $\mu$ )	VA (LogMAR)
Outer retinal atrophy	$29.3 \pm 18.1$	$156 \pm 44$	$0.96 \pm 0.39$
Undifferentiated outer retinal layers	$18.3 \pm 14.2$	$217 \pm 27$	$0.87 \pm 0.31$
Ellipsoid zone disruption	$9.3 \pm 4.2$	$176 \pm 51$	$0.71 \pm 0.40$
Outer foveal defect	$32.3 \pm 14.0$	$233 \pm 44$	$0.70 \pm 0.33$
Prominent outer retinal layers	$15.1 \pm 6.8$	$194 \pm 44$	$0.65 \pm 0.33$
p-value <sup>a</sup>	$< 0.001$	$< 0.001$	0.16
<sup>a</sup> Calculated by generalized estimating equations analysis			
CST = central subfoveal thickness; VA = visual acuity			

EZ disruption group had the lowest mean age among the other groups ( $9.3 \pm 4.2$ ;  $p < 0.01$ ), while outer foveal defect group had the highest mean age ( $32.3 \pm 14.0$ ;  $p < 0.01$ ). CST was greater in outer foveal defect group ( $233 \pm 44\mu$ ), followed by prominent outer retinal layers group ( $217 \pm 27\mu$ ). In pairwise comparison, these two groups had significantly higher CRT compared to that of the outer retinal atrophy group, the group with the smallest CST ( $156 \pm 44\mu$ ). ( $p < 0.001$ ). No association was found between CST and VA in univariate GEE analysis ( $p = 0.17$ ).

The five isolated signs and their associations with the five major categories of abnormal structural morphologies were additionally studied (Table 2). THD and pseudodrusen were seen significantly more in the outer retinal atrophy group ( $p = 0.033$  and  $p < 0.001$ , respectively), while foveal hypoplasia was seen more in the EZ disruption and outer foveal defect groups ( $p < 0.01$ ). OPL schisis was most common in the EZ disruption group ( $p < 0.05$ ). EZ bowing presence was evenly distributed amongst the morphological groups ( $p = 0.11$ ).

Table 2  
Bivariate analysis of major morphological categories and isolated signs.

	Total cases	FH	THD	OPL schisis	Pseudodrusen	EZ bowing
Outer retinal atrophy	20 (24.40%)	0	9(45%)	0	7 (35%)	1(5%)
Undifferentiated outer retinal layers	18 (22.0%)	0	7 (36.9%)	1 (5.5%)	0	0
EZ disruption	16 (19.5%)	6 (37.5%)	0	6(37.5%)	0	3(18.7%)
Outer foveal defect	14 (17.1%)	4 (28.6%)	5(36.7%)	2 (14.2%)	1 (7.1%)	3 (21.4%)
prominent outer retinal layers	14 (17.1%)	2(14.2%)	3(21.4%)	0	0	4(28.5%)
Total	82 (100%)	12 (14.6%)	24(29.3%)	9 (11.3%)	8 (9.8%)	11(13.4%)
p-value <sup>a</sup>		0.003	0.033	0.044	0.001	0.113
<sup>a</sup> Calculated by chi-square analysis						
EZ = ellipsoid zone; FH = foveal hypoplasia; THD = transretinal hyper-reflective dots; OPL = outer plexiform layer						

A multivariate GEE regression analysis was performed to ascertain any possible relationship between VA and other factors. Similar to univariate analysis which revealed no significant relationship between VA and morphological categories ( $p = 0.16$ ), multivariate GEE analysis revealed no association between VA and age, thickness, or morphological category ( $p = 0.83, 0.30, \text{ and } 0.32$ , respectively).

## Discussion

In this study we assessed SD-OCT images of 84 eyes from 42 patients with cone dystrophy. Among those patients, 82 eyes had SD-OCT abnormalities. We categorized the ocular structural abnormalities of these patients in order to search for a correlation between the structural changes and VA. We classified the observed structural abnormalities into two generalized categories: 1. Abnormalities of outer retina hyper-reflective bands that seemed to be major and were categorized into 5 groups; 2. Isolated OCT abnormality

signs. The five-overarching major morphological groups include (1) outer retinal atrophy, (2) undifferentiated outer retinal layers, (3) EZ disruption, (4) outer foveal defect, and (5) prominent outer retinal layers. The isolated signs were foveal hypoplasia, THD, OPL schisis, pseudodrusen, and EZ bowing.

In the literature, there have been only few published manuscripts evaluating cone dystrophy eyes using SD-OCT imaging. Cho et al. published a series describing the SD-OCT findings of 15 patients with cone dystrophy.<sup>8</sup> They categorized findings into four groups based on the status of EZ, OS contact cylinder or IZ, and RPE: Category 0 included no abnormality, category 1 included foveal EZ loss and obscurity of the border between the EZ band and ELM, category 2 included foveal thinning and focal foveal EZ disruption with an intact ELM, and category 3 included foveal thickening with perifoveal disruption of the EZ. Categories 1–3 all had thickening of RPE and absence of IZ in common. In the study by Cho et al., 4 out of 15 patients (aged 7, 9, 11, and 13 years) had normal retinal findings on OCT, while in our study only two out of 84 eyes (42 patients) had normal retinal findings on SD-OCT. One reason for this could be that our tertiary referral center sees patients with more advanced diseases who are referred. Additionally, only patients with severely reduced or non-recordable cone responses were included in our study. This is opposed to the Cho et al. study which included cone dystrophy patients with recorded photopic and 30-Hz flicker responses that were lower than those of the normal control group ( $p < 0.001$ ) but not severely reduced or non-recordable.

Our findings demonstrate the applicability and utility of SD-OCT imaging in the diagnosis of cone dystrophy patients. In our larger series of 42 patients, some detected SD-OCT abnormalities were difficult to classify into the four categories described by Cho et al.<sup>8</sup> Additionally, the abnormalities we identified exhibited distinct characteristics and morphological patterns, prompting us to propose the five overarching morphological patterns described above.

Patients in the first category had atrophy of outer retinal layers, resulting in diffuse or outward disfiguration of the outer retinal layers, resembling a waterfall pattern. Outer retinal atrophy may be the endpoint of different retinal diseases and dystrophies, indicating its utility as a prognostic OCT biomarker and may be correlated with VA.

Sergouniotis et al. reviewed SD-OCT images of 12 patients with cone dystrophy with supernormal rod electroretinogram due to the KCNV2 gene.<sup>10</sup> They found that four patients had lost all or nearly all of their outer retinal layers in the foveal region. They observed increased autofluorescence in three patients' paracentral ring and one patient's central fovea. The visual acuity of these patients was lower than the others 8 patients included in the study. However, statistical analysis was not performed due to the small sample size of patients assessed.<sup>10</sup> Mizobuchi et al. reported 9 patients with cone/cone-rod dystrophy who carried the GUCA1A mutation.<sup>11</sup> They found diffuse outer retinal atrophy in four patients, one of whom had outward disfiguration of the retina as we described. Although the VA was lower in patients with atrophy and thinning of outer retinal layers compared to control, the sample size was small and statistical analysis was not performed.<sup>10,11</sup>



The second category, undifferentiated outer retinal layers, demonstrated diminished signals of outer hyper-reflective retinal bands with integration of some or all bands, giving the appearance of hatched pattern. Hood et al. hypothesized that a decrease in the EZ intensity is associated with achromatopsia and cone dystrophy.<sup>7</sup>

The third category that we described consisted of patients with scattered EZ disruption. Similarly, Xu et al. reported a cone dystrophy patient with longstanding bilateral vision loss and photophobia who had central loss of the inner segment of EZ.<sup>12</sup> Similar findings were discovered in his sister and maternal aunt. In that case, cone dystrophy was associated with the KCNV2 mutation. Additionally, his VA remained stable over the two-year follow-up period. Manes et al. reported a family carrying the GUCA1A mutation. From adolescence, one of the family members experienced vision loss and photophobia.<sup>13</sup> This patient's disease progressed further later in adulthood. SD-OCT imaging of that patient demonstrated EZ loss with ONL thinning. Fundoscopic examination showed macular atrophy with granular deposits in the macular region.<sup>13</sup> Eight of 12 patients reported by Sergouniotis et al. had loss of EZ band in the foveal region, accompanied by a significant decrease in visual acuity.<sup>10</sup>

The fourth category was outer foveal defect, which was detected in the subfoveal segment of 14 patients. This category was consistent with the fourth category described by Sundaram et al.: achromatopsia structural abnormality on SD-OCT imaging.<sup>14</sup> Furthermore, Hirji et al. reported 50 patients with achromatopsia who had retinas that remained structurally stable over a mean follow-up period of 61.6 months.<sup>15</sup> However, 2 patients in that study had focal disruption of EZ that progressed to optically empty spaces in the outer retina.<sup>15</sup> Leng et al. described this structural abnormality as "foveal cavitation".<sup>16</sup> The authors also reported abnormalities in the desaturated color vision testing of all 8 patients.<sup>16</sup>

The final category was prominent outer retinal layers which was found in 14 eyes in the present study. Unlike the other four groups with varied degrees of attenuation, loss, disruption and reduced reflectivity of outer retinal hyperreflective bands, this group manifested with distinct OCT features. The outer retinal layers are preserved and appear to be thickened and more hyperreflective. Duncan et al. reported 4 patients with cone-rod dystrophy who had heterozygote point mutations in the peripherin/RDS gene.<sup>17</sup> Their SD-OCT imaging showed extensive loss of the outer nuclear, inner segment, and outer segment layers in the central macula. However, at the fovea, outer retinal structures were relatively well preserved and hyperreflective, but irregular structures were present in all patient's outer segment-RPE junction layer, giving the appearance of outer retinal layer thickening. This hyper-reflective layer had minimal abnormality in patient 1, who had better visual function than others despite having a cone-rod dystrophy phenotype based on full-field ERG testing. Microperimetry showed a 1 to 2 log unit reduction in sensitivity throughout the central 8°. <sup>17</sup> In another case report of occult macular dystrophy, SD-OCT imaging of outer retinal layers in the central area demonstrated local thickening. Multifocal ERG testing showed reduced amplitudes in the central ring of both eyes, with normal scotopic and photopic full-field ERG responses.<sup>18</sup> However, in our patients, preserved and prominent hyperreflective outer retinal layers were more diffuse, distinct, and did not show disruption of adjacent outer retinal layers. To the best of our knowledge, this

feature has not been previously reported in patients with cone dystrophy. We hypothesize that it is a result of photoreceptor maldevelopment.

In our study, we also reported the following isolated SD-OCT features: foveal hypoplasia, THD, OPL schisis, pseudodrusen, and EZ bowing. While foveal hypoplasia is a common finding in achromatopsia, to our knowledge, the remaining four signs have not been reported.

THD was the most frequent isolated OCT sign in the present study. Hyper-reflective dot (HD) or foci have been reported frequently in diabetic macular edema,<sup>19</sup> retinal vein occlusion,<sup>20</sup> and exudative age-related macular degeneration (wet-AMD).<sup>21</sup> According to some authors, the presence of HDs may affect the prognosis and treatment decision in these patients.<sup>20,21</sup> Pseudodrusen, also known as subretinal drusenoid deposit, is also frequently observed in AMD patients, and its presence has been linked to a significantly increased risk of AMD progression, progressive outer retinal degeneration, and reduced retinal sensitivity on microperimetry testing.<sup>22</sup> Severe rod dysfunction was also noted in retinal areas covered with pseudodrusen.<sup>23</sup> Interestingly, THD and pseudodrusen were both present in our cone dystrophy cases; however, it is unknown whether the presence of these SD-OCT signs affects the natural disease progression of cone dystrophy.

OPL schisis was detected in 9 (11.3%) eyes in the index study. It is a distinct and interesting OCT feature that may reflect anatomical variation.

EZ bowing was another interesting and distinct finding, featuring localized central displacement or bending of the EZ towards the ILM. It may be related but is morphologically distinct from outer foveal defect with the absence of EZ. In our study, EZ bowing was present in 11 (13.4%) eyes. It may possibly indicate the anatomical disarrangement of cone cells.

In this study, the identified major morphological classifications were associated with patients' ages. EZ disruption and prominent outer retina morphologies were more commonly seen in younger patients (1st and 2nd decades of life), and outer foveal defect was more commonly seen in older patients (3rd through 6th decades of life). In contrast, Cho et al. reported that there was no statistically significant difference between the age of categories proposed in their study.<sup>8</sup>

According to the literature, each of the different genetic variants of cone dystrophy has its own distinct mechanism, pathophysiology, and natural disease course.<sup>1</sup> Hence, it is possible that the various morphological patterns we have seen may be associated with distinct types of cone metabolism pathways and associated dysfunction. Unfortunately, there is currently no information available about the genetic status of the patients in these series.

In univariate and multivariate analyses, there was no correlation between VA and the different morphological alterations on SD-OCT. However, morphological classification was associated with CST; the outer foveal defect group had higher CST values and the outer retinal atrophy group had lower CST values in comparison to other groups. In contrast to our findings, Cho et al. reported that in cases with

retinal abnormalities detected using SD-OCT, the CST and ONL were thinner and the RPE was thicker compared to cases without detectable abnormalities (category 0).<sup>8</sup> Additionally, they reported a significant correlation between CST and VA in cone dystrophy patients<sup>8</sup>, whereas no correlation between CST and VA was found in the index study.

Our study does have few limitations. It should be noted that sample size of the present study may still be insufficient to detect differences statistically. However, sample size is still larger as compared to the previous studies. In addition to lack of genetic test results, the other limitation of our study was its retrospective design which limited access to relevant data such as symptoms duration and family history. Additionally, each patient's paired eyes were categorized similarly, indicating a probable source of bias in analysis that was compensated for by the GEE method.

In conclusion, the index study with SD-OCT imaging have demonstrated a variety of morphologic findings in cone dystrophy, which may be employed in the assessment of these patients and may serve as predictive biomarkers for visual outcomes and clinical course.

## Declarations

### Acknowledgement

The author(s) do not have any conflict of interests to disclose and did not receive any financial support for the research, authorship, and/or publication of this article.

## References

1. Roosing S, Thiadens AA, Hoyng CB, Klaver CC, den Hollander AI, Cremers FP. Causes and consequences of inherited cone disorders. *Progress in retinal and eye research*. 2014;42:1-26.
2. Thiadens AA, Phan TML, Zekveld-Vroon RC, et al. Clinical course, genetic etiology, and visual outcome in cone and cone-rod dystrophy. *Ophthalmology*. 2012;119(4):819-826.
3. Berger W, Kloeckener-Gruissem B, Neidhardt J. The molecular basis of human retinal and vitreoretinal diseases. *Progress in retinal and eye research*. 2010;29(5):335-375.
4. Forte R, Cennamo G, Finelli M, De Crecchio G. Comparison of time domain Stratus OCT and spectral domain SLO/OCT for assessment of macular thickness and volume. *Eye*. 2009;23(11):2071-2078.
5. Lima LH, Sallum JM, Spaide RF. Outer retina analysis by optical coherence tomography in cone-rod dystrophy patients. *Retina*. 2013;33(9):1877-1880.
6. Watanabe SE, Passos R, Castro AR, Sacai PY, Salomão SR, Berezovsky A. High Resolution Optical Coherence Tomography in Retinal Dystrophy. *Investigative Ophthalmology & Visual Science*. 2011;52(14):3205-3205.
7. Hood DC, Zhang X, Ramachandran R, et al. The inner segment/outer segment border seen on optical coherence tomography is less intense in patients with diminished cone function. *Investigative*

- ophthalmology & visual science*. 2011;52(13):9703-9709.
8. Cho SC, Woo SJ, Park KH, Hwang J-M. Morphologic characteristics of the outer retina in cone dystrophy on spectral-domain optical coherence tomography. *Korean Journal of Ophthalmology*. 2013;27(1):19-27.
  9. McCulloch DL, Marmor MF, Brigell MG, et al. ISCEV Standard for full-field clinical electroretinography (2015 update). *Documenta ophthalmologica*. 2015;130(1):1-12.
  10. Sergouniotis PI, Holder GE, Robson AG, Michaelides M, Webster AR, Moore AT. High-resolution optical coherence tomography imaging in KCNV2 retinopathy. *British journal of ophthalmology*. 2012;96(2):213-217.
  11. Mizobuchi K, Hayashi T, Katagiri S, et al. Characterization of GUCA1A-associated dominant cone/cone-rod dystrophy: low prevalence among Japanese patients with inherited retinal dystrophies. *Scientific reports*. 2019;9(1):1-9.
  12. Xu D, Su D, Nusinowitz S, Sarraf D. Central ellipsoid loss associated with cone dystrophy and KCNV2 mutation. *Retinal Cases and Brief Reports*. 2018;12:S59-S62.
  13. Manes G, Mamouni S, Hérald E, et al. Cone dystrophy or macular dystrophy associated with novel autosomal dominant GUCA1A mutations. *Molecular Vision*. 2017;23:198.
  14. Sundaram V, Wilde C, Aboshiha J, et al. Retinal structure and function in achromatopsia: implications for gene therapy. *Ophthalmology*. 2014;121(1):234-245.
  15. Hirji N, Georgiou M, Kalitzeos A, et al. Longitudinal assessment of retinal structure in achromatopsia patients with long-term follow-up. *Investigative ophthalmology & visual science*. 2018;59(15):5735-5744.
  16. Leng T, Marmor MF, Kellner U, et al. Foveal cavitation as an optical coherence tomography finding in central cone dysfunction. *Retina*. 2012;32(7):1411-1419.
  17. Duncan JL, Talcott KE, Ratnam K, et al. Cone structure in retinal degeneration associated with mutations in the peripherin/RDS gene. *Investigative Ophthalmology & Visual Science*. 2011;52(3):1557-1566.
  18. Tojo N, Nakamura T, Ozaki H, Oka M, Oiwake T, Hayashi A. Analysis of macular cone photoreceptors in a case of occult macular dystrophy. *Clinical Ophthalmology (Auckland, NZ)*. 2013;7:859.
  19. Bolz M, Schmidt-Erfurth U, Deak G, et al. Optical coherence tomographic hyperreflective foci: a morphologic sign of lipid extravasation in diabetic macular edema. *Ophthalmology*. 2009;116(5):914-920.
  20. Ogino K, Murakami T, Tsujikawa A, et al. Characteristics of optical coherence tomographic hyperreflective foci in retinal vein occlusion. *Retina*. 2012;32(1):77-85.
  21. Coscas G, De Benedetto U, Coscas F, et al. Hyperreflective dots: a new spectral-domain optical coherence tomography entity for follow-up and prognosis in exudative age-related macular degeneration. *Ophthalmologica*. 2013;229(1):32-37.

22. Holz FG, Saßmannshausen M. Reticular Pseudodrusen: Detecting a Common High-Risk Feature in Age-Related Macular Degeneration. *Ophthalmology Retina*. 2021;5(8):719-720.
23. Steinberg JS, Fitzke FW, Fimmers R, Fleckenstein M, Holz FG, Schmitz-Valckenberg S. Scotopic and photopic microperimetry in patients with reticular drusen and age-related macular degeneration. *JAMA ophthalmology*. 2015;133(6):690-697.

## Figures

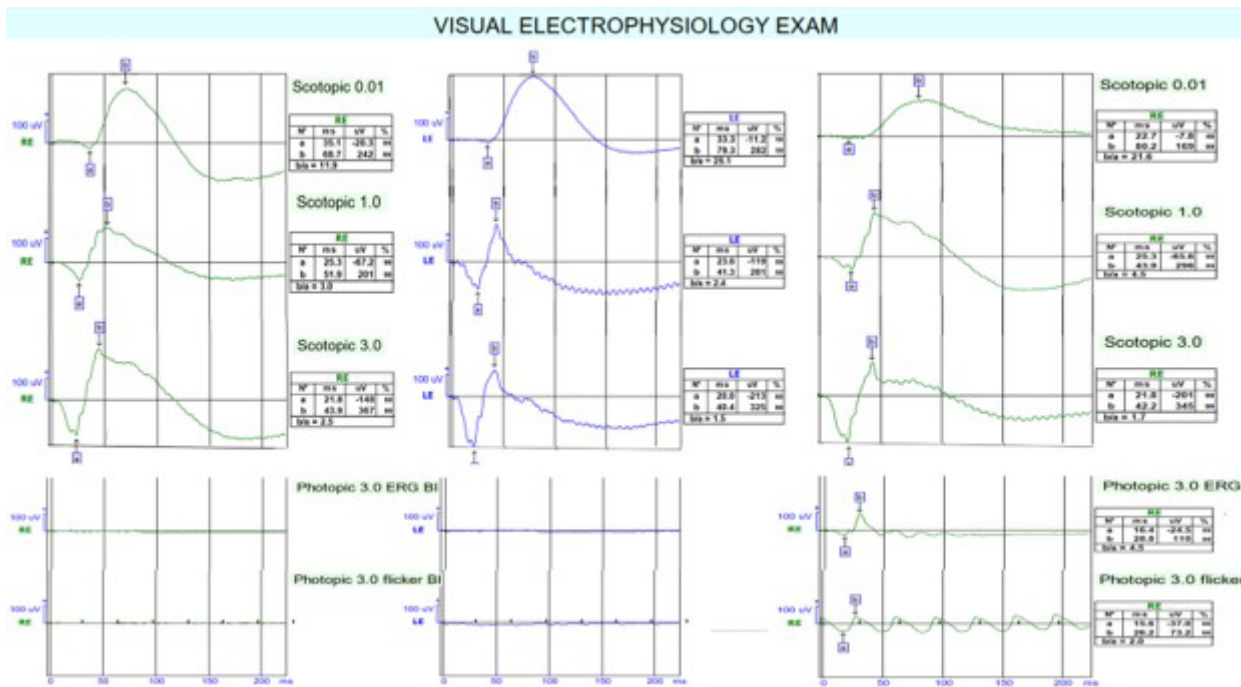


**Figure 1**

Full-field electroretinogram (Full-field ERG) shows similar intact scotopic responses in a patient with cone dystrophy with severely reduced photopic responses, and a normal subject (left and middle columns: right and left eyes of a cone dystrophic patient; right column: full-field ERG of a subject with no known ocular diseases).

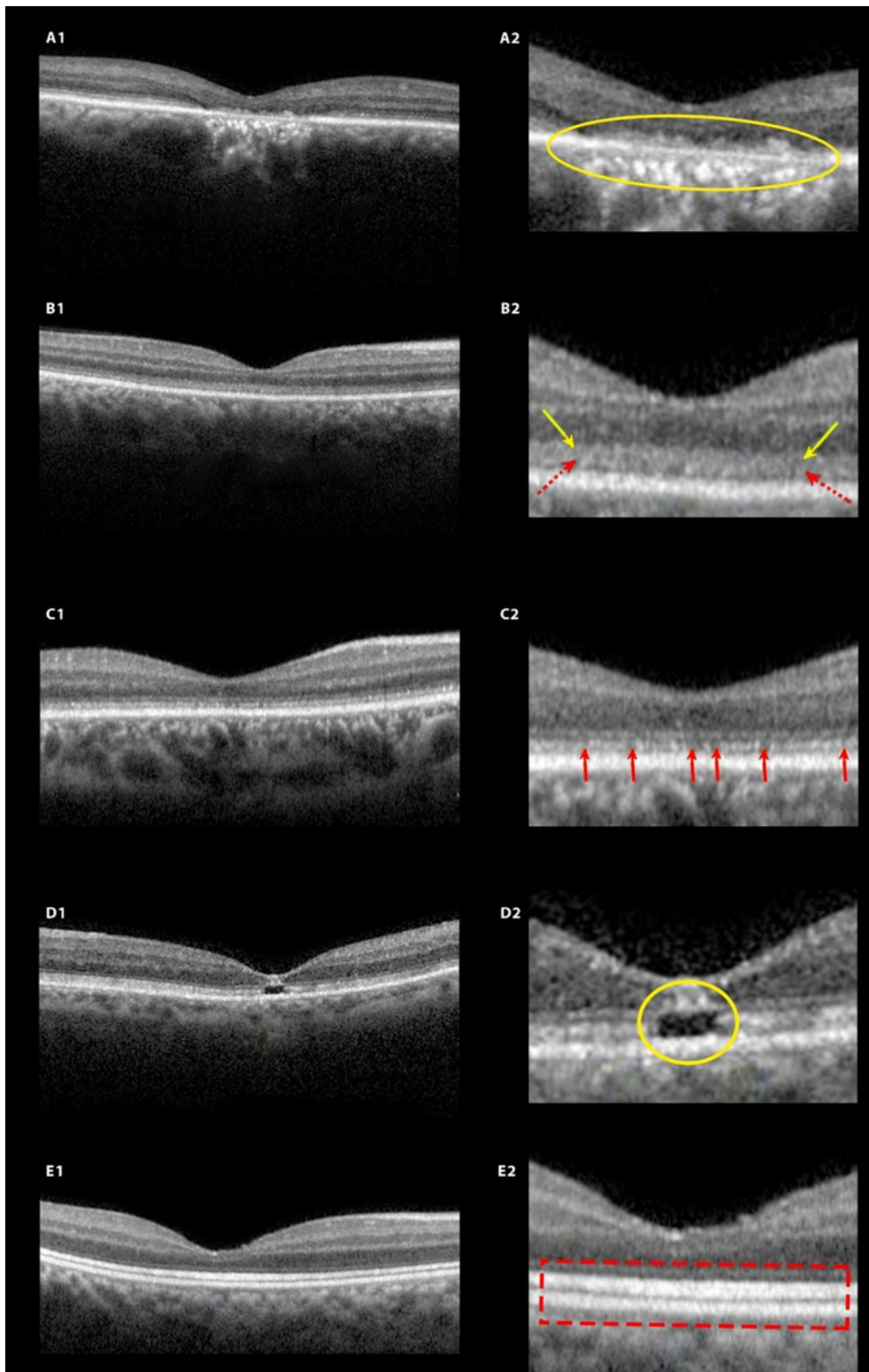


**Figure 2**

Five morphological SD-OCT features of cone dystrophy based on outer retinal layers patterns (magnified view included in right column). A1-2: Outer retinal atrophy—loss of ELM and EZ with outward disfiguration of retinal layers (yellow ellipsoid). B1-2: Undifferentiated outer retinal layers—the ELM (yellow arrows) and EZ (red dashed arrows) are merged so that boundaries cannot be well distinguished. C1-2: EZ disruption—scattered disruptions of the EZ (red arrows). D1-2: Outer foveal defect—localized

attenuation or loss of EZ at fovea creating a micro defect (yellow circle). E1-2: Prominent outer retinal layers—outer retinal layers are well preserved and prominently hyperreflective (dashed red box).

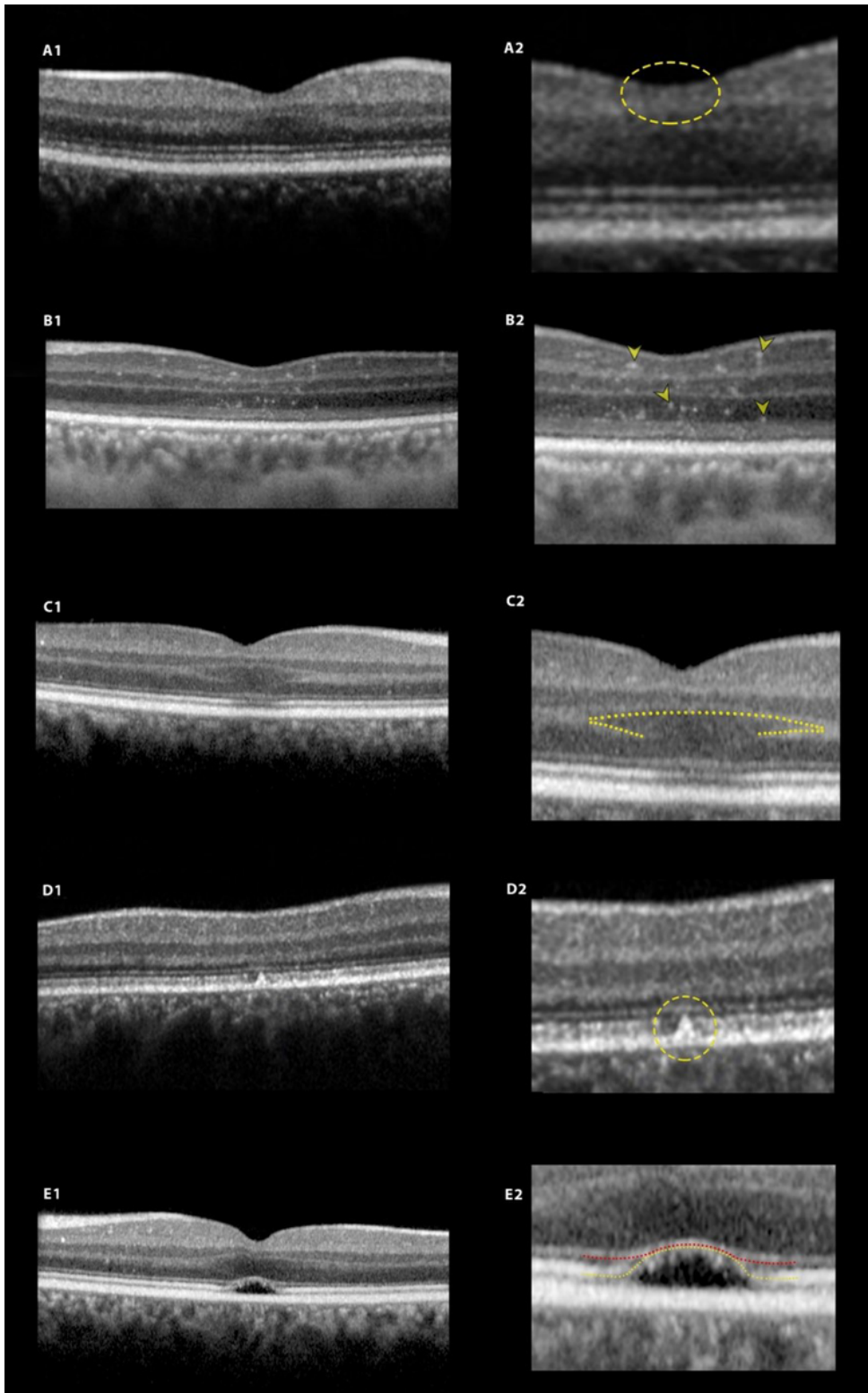


**Figure 3**

Isolated SD-OCT features in cone dystrophy (magnified view included in right column). A1-2: Foveal hypoplasia—abnormal presence of inner retinal layers at the fovea (dashed yellow ellipse). B1-2: Trans

retinal hyperreflective dots (THD) –diffuse hyperreflective foci in neurosensory retina (yellow arrow heads). C1-2: OPL schisis (yellow dashed line). D1-2: Pseudodrusen –hyperreflective deposits above the RPE (yellow circle). E1-2: EZ bowing-central EZ (dashed yellow line) is displaced towards ELM (red dashed line).